Electrostatic Properties of Myoglobin Probed by Diffusion-Enhanced Energy Transfer†

Theodore G. Wensel and Claude F. Meares*

ABSTRACT: The use of lanthanide energy transfer in the "rapid-diffusion limit" for probing the electrostatic properties of proteins has been investigated by measuring rates of energy transfer from Tb(III) chelates (having charges 1+, 0, and 1−) to the heme of sperm whale met(aquo)myoglobin, as a function of pH. The results are in good agreement with the predictions of a simple model involving the overall charge of the protein. The preparation of terbium(III) *N*,*N*′-bis(2-hydroxyethyl)-ethylenediaminediacetate, a new positively charged Tb(III) chelate similar in size and shape to negative terbium(III) ethylenediaminetetraacetate and neutral terbium(III) *N*-(2-hydroxyethyl)ethylenediaminetriacetate, is described.

Diffusion-enhanced energy transfer [Thomas et al., 1979; for a review, see Stryer et al. (1982a)] from lanthanide chelates has been successfully used to measure the accessibility of macromolecular chromophores to small molecules in solution (Yeh & Meares, 1980; Meares & Rice, 1981; Thomas & Stryer, 1982; Rice & Meares, 1982). This technique is based on the fact that intermolecular energy transfer is enhanced by diffusion when the lifetime of the donor's excited state is longer than the time required for the donor–acceptor separation to change significantly. Energy transfer is maximally enhanced at the rapid-diffusion limit, where the distance diffused by an excited donor during its lifetime is much greater than the average distance between acceptors. This situation is easily achieved with lanthanide chelates (lifetime $\simeq 10^{-3}$ s), and acceptor concentrations greater than micromolar in aqueous solution at 25 °C (Thomas et al., 1979; Yeh & Meares, 1980). Under these conditions, the rate of energy transfer is strongly dependent on the *distance of closest approach* between donor and acceptor.

A potentially useful feature of diffusion-enhanced energy transfer, which has not yet been thoroughly characterized, is its sensitivity to electrostatic effects (Meares et al., 1981; Yeh & Meares, 1980; Stryer et al., 1982b). Electrostatic properties are important in the interaction of many proteins with other molecules (e.g., other proteins, membranes, nucleic acids, substrates, and effectors), and a nonperturbing method for directly monitoring these properties could have many applications.

In the rapid-diffusion limit, a typical energy donor encounters hundreds of possible acceptors and passes through much of the solution surrounding each. Thus, the rate of energy transfer is dependent on the time-averaged, quasi-equilibrium distribution of donors about an acceptor (or vice versa). This distribution, in turn, is strongly influenced by electric charges on the donor and acceptor. Thus, the rates of energy transfer from charged donors can be either lower or higher than the rates of energy transfer from a neutral donor, depending on the sign and magnitude of the electrostatic potential near the energy acceptor.

In order to probe the electrostatic potentials about chromophores of biological interest, we have prepared a series of Tb(III) chelates with different charges, but similar sizes and shapes. Here we describe the synthesis of TbBED2A$^+$ [1] (Figure 1c), the Tb(III) chelate of *N*,*N*′-bis(2-hydroxyethyl)ethylenediaminediacetate (Chaberek & Bersworth, 1953). This new complex serves as a positively charged energy transfer probe whose size and shape are similar to those of negative TbEDTA$^-$ (Figure 1a) and neutral TbHED3A (Figure 1b). The use of two oppositely charged probes in addition to the neutral probe provides a useful cross-check on experimental results.

For our initial investigations of electrostatic effects, we chose the heme protein myoglobin. The visible absorbance of the heme prosthetic group makes it a good energy acceptor for Tb(III) chelates (Figure 2). In addition, the electrostatic properties of myoglobin have been the subject of extensive study (e.g., Shire et al., 1974a,b; Friend & Gurd, 1979; Matthew et al., 1978). Its acid–base titration behavior allows changing the protein's net charge considerably, without bringings about gross structural changes, in the pH range from 6 to 8.5. As described below, the results obtained with this well-characterized protein provide a basis for diffusion-enhanced energy transfer studies of more complex systems.

Theory

Energy transfer between electrically charged chelates and globular proteins may be simply modeled as an interaction between two electrically charged spheres of uniform surface charge density (see Figure 3; the validity of this approximation will be discussed below). The effect of charge interactions is to alter the equilibrium distribution of donor ions about the protein, relative to the distribution of a neutral species of the same size and concentration. The local concentration of donor ions at a distance r from the center of the protein can be approximated as the product of the bulk concentration of the donor and a Boltzmann factor, $\exp[-w(r)/(kT)]$ (Olivares & McQuarrie, 1975). Here, $w(r)$ is the potential of mean force (discussed below) between the donor and acceptor, k is Boltzmann's constant, and T is the absolute temperature.

Energy transfer can occur by several physical mechanisms (Förster, 1948; Dexter, 1953). The dipole–dipole mechanism operates through space and is dependent on the inverse sixth power of the donor–acceptor separation. The exchange mechanism requires collision, so the rate of energy transfer

† From the Chemistry Department, University of California, Davis, California 95616. *Received May 13, 1983.* Supported by Research Grants GM25909 and CA16861 and Research Career Development Award CA00462 to C.F.M. from the National Institutes of Health, by Chemical Research Instrumentation Grant CHE8114966 to the Chemistry Department from the National Science Foundation, and by a Graduate Fellowship to T.G.W. from the University of California, Davis.

[1] Abbreviations: EDTA, ethylenediaminetetraacetic acid; TbEDTA$^-$, the Tb(III) complex of EDTA; CoEDTA$^-$, the Co(III) complex of EDTA; HED3A, *N*-(2-hydroxyethyl)ethylenediaminetriacetic acid; TbHED3A, the Tb(III) chelate of HED3A; BED2A, *N*,*N*′-bis(2-hydroxyethyl)ethylenediaminediacetic acid; TbBED2A$^+$, the Tb(III) chelate of BED2A; en, ethylenediamine.

0006-2960/83/0422-6247$01.50/0

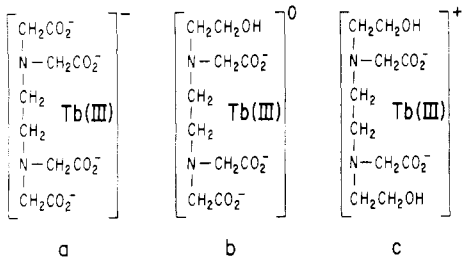

FIGURE 1: Structures of Tb(III) chelates used as energy transfer probes. (a) TbEDTA$^-$; (b) TbHED3A; (c) TbBED2A$^+$.

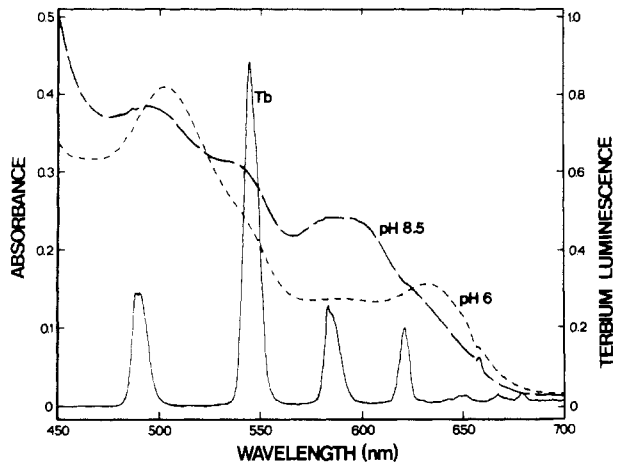

FIGURE 2: Spectral overlap of Tb(III) emission and myoglobin absorbance. (---) Absorbance of 43.4 mM met(aquo)myoglobin, pH 6.0; (--) absorbance of 43.4 mM met(aquo)myoglobin, pH 8.5; (—) corrected emission spectrum of TbHED3A, excited at 352 nm.

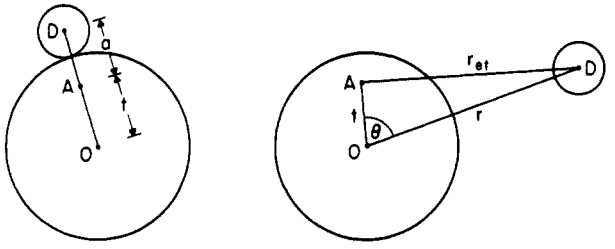

FIGURE 3: Model of interaction between donor chelates and protein in diffusion-enhanced energy transfer. Both the donor and the protein are considered as impenetrable spheres. A indicates the acceptor and D the donor chelate. The quantity a denotes the distance of closest approach between D and A. The distance from the center of the protein to A is denoted by t. The quantity $(t + a)$ represents the distance of closest approach between D and the center of the protein, which is assumed to be the center of its electric charge. At any point in solution occupied by the donor, the distance between the donor and acceptor is r_{et}, and the distance between the donor and the center of the protein is r.

by exchange is proportional to $\exp(-2r_{et}/l)$, where r_{et} is the donor–acceptor separation and l is an effective average atomic radius. Other mechanisms of energy transfer are probably less important (Dexter, 1953).

The second-order rate constant for dipole–dipole energy transfer in the rapid-diffusion limit is obtained by integrating r_{et}^{-6} over all the space around the acceptor which is available to the donor. If we model the heme in myoglobin as an acceptor located off the center of an impenetrable sphere, then (if there are no electrostatic effects) the second-order rate constant k_2 is given by

$$k_2 = 0.6023 \frac{R_0^6}{\tau_0} \int\int\int r_{et}^{-6}\, dV \ \mathrm{M^{-1}\ s^{-1}} \qquad (1)$$

Here R_0 is the distance (nm) at which energy transfer is 50% efficient (Förster, 1948), τ_0 (s) is the donor excited-state lifetime in the absence of acceptor, and r_{et} is the distance (nm) from the donor to the acceptor. The integration is over all the space available to the donor (Figure 3).

R_0 may be calculated from measured properties of the donor emission and the acceptor absorption spectra according to

$$R_0 = 979(JQ_0\kappa_{or}^2 n^{-4})^{1/6}\ \mathrm{nm} \qquad (2)$$

$$J = \frac{\int F(\lambda)\epsilon(\lambda)\lambda^4\, d\lambda}{\int F(\lambda)\, d\lambda} \qquad (3)$$

where J is the spectral overlap integral, $F(\lambda)$ is the relative fluorescence intensity of the donor at wavelength λ, and $\epsilon(\lambda)$ is the molar extinction coefficient of the acceptor at the same wavelength. Q_0 is the quantum yield of the donor in the absence of acceptor, κ_{or}^2 is the orientation factor between the transition dipoles (assumed to be $^2/_3$ in this case; Thomas et al., 1979), and n is the refractive index of the intervening medium. For TbEDTA$^-$ and met(aquo)myoglobin, R_0 is between 3.4 and 3.5 nm, depending on pH (see Figure 2).

If the radii of both probe (R_D) and protein (R_A) are known, then since $R_A + R_D = a + t$, values of a and t can be calculated from the rate constant for the neutral probe according to Stryer et al. (1982a):

$$k_2 = 0.6054\pi R_0^6(1/\tau_0)a^{-3}[2 - [a/(a + t)]]^{-3} \qquad (4)$$

The value of k_2 for the neutral probe is a measure of the chromophore's accessibility.

In order to account for electrostatic effects, it is necessary to multiply the integrand in eq 1 by the factor $\exp[-w(r)/(kT)]$. For small 1–1 and 2–2 electrolytes up to a concentration of 1 M, the potential of mean force is closely approximated by (Olivares & McQuarrie, 1975)

$$w(r) = \frac{Z_A Z_D e^2 \exp[-\kappa[r - (R_A + R_D)]]}{\epsilon[1 + \kappa(R_A + R_D)]r} \qquad (5)$$

where Z_A is the acceptor charge, Z_D is the donor charge, e is the electron charge, ϵ is the dielectric constant, and κ is the Debye–Hückel parameter, which is $3.3I^{1/2}$ nm^{-1} in water at 298 K (I is the ionic strength). If Z_A is known, comparison between experimental results and the rate constants predicted by eq 1–5 provides a test of the applicability of this simple model for analyzing protein electrostatics. Conversely these relations may be used to determine Z_A.

A somewhat different approach involves approximate solutions to the nonlinear Poisson–Boltzmann equation. Although it is known to have limited validity for simple electrolyte solutions (Olivares & McQuarrie, 1975), this equation has been useful in describing the electrostatic properties of charged surfaces and particles and of polyelectrolytes (Rice & Nagasawa, 1961; Scheraga et al., 1969; McLaughlin, 1977; McClanahan, 1982). An analytic formula which provides results in good agreement with detailed numerical solutions of the nonlinear Poisson–Boltzmann equation for charged particles in electrolyte solutions has been reported by Ohshima et al. (1982). Their paper yields an analytic expression for the potential, $\psi(r)$ (see Appendix). The expression

$$w(r) = Z_D e\psi(r) \qquad (6)$$

may be used as an alternative to eq 5.

In the case of energy transfer by the exchange interaction, electrostatic effects are closely approximated by (Meares et al., 1981)

$$k_2 = k_0 \exp[-w(R_A + R_D)/(kT)] \qquad (7)$$

where k_0 is the rate constant for energy transfer from the

neutral probe. For the dipolar case

$$k_2 = \frac{0.6023R_0^6}{\tau_0}\int\int\int e^{-w(r)/(kT)} r_{et}^{-6}\, dV \qquad (8)$$

and numerical integration (see Appendix) is required.

Experimental Procedures

Materials. Unless otherwise specified, all chemicals used were reagent grade. All labware was acid washed to remove trace metal ions. All water used was deionized and glass distilled.

Synthesis of N,N'-Bis(2-hydroxyethyl)ethylenediaminediacetic Acid. A total of 5.0 g (33.8 mmol) of *N,N'*-bis(2-hydroxyethyl)ethylenediamine (Alfa) was dissolved in 10 mL of H_2O and adjusted to pH 11 with 7 N KOH. A total of 10.0 g (72 mmol) of $BrCH_2COOH$ (Aldrich; recrystallized from hexane) was added slowly, while the pH was maintained between 10 and 11 with KOH. The mixture was stirred at 40 °C overnight. For the first few hours pH was monitored and maintained continuously until it stabilized.

A slight excess of $CuCl_2$ was added to form the Cu(II) complex. Thin-layer chromatography of the complex (silica gel 60; E. Merck), developed with a 7/3 (v/v) mixture of 95% ethanol and 14 M NH_4OH, gave a blue spot at R_f 0.4, while a mixture of starting material and $CuCl_2$ gave only a blue spot at the origin.

An aliquot of the reaction mixture containing Cu(II) was applied to a 1 × 45 cm AG-50 column (NH_4^+ form; Bio-Rad) and washed through with water. The pH of the flow through was lowered to 2.0, and the solution was extracted several times with diethyl ether to remove excess $BrCH_2COOH$. Alternatively, the extraction was performed before the chromatography, and an additional step of washing the product through an AG-1 column (formate form; Bio-Rad) with H_2O was employed to remove nonvolatile anions. The resulting solution which contained purified Cu(II)BED2A was treated with H_2S to remove Cu(II), boiled to coagulate the precipitate, and filtered several times through paper (Schleicher & Schuell no. 588).

The filtrate was lyophilized and dissolved in D_2O, and the resulting solution was adjusted to a pH meter reading of 9.0. The NMR spectrum of the product BED2A contained a triplet (4 H) at 2.95 ppm, a singlet (4 H) at 3.1 ppm, a singlet (4 H) at 3.5 ppm, and a triplet (4 H) at 3.8 ppm (based on HOD peak at 4.8 ppm), while the spectrum of the starting material *N,N'*-bis(2-hydroxyethyl)ethylenediamine contained a superimposed triplet (4 H) and singlet (4 H) at 2.65 ppm and a triplet (4 H) at 3.8 ppm.

The BED2A chelate of Tb(III) was formed by adding 1.42 g (3.8 mmol) of $TbCl_3 \cdot 6H_2O$ (Alfa) to 1 g (3.8 mmol) of BED2A and adjusting to pH 7 with NH_4OH. This solution was chromatographed on a 2.6 × 22 cm AG-50 column (NH_4^+ form) by using a 500-mL linear ammonium acetate gradient, 0.0–1.0 M, at pH 7. The main peak, as detected by Tb(III) luminescence (λ_{ex} 244 nm, λ_{em} 546 nm; Perkin-Elmer MPF44B fluorescence spectrophotometer), was eluted at concentrations between 0.65 and 0.75 M NH_4OAc and lyophilized.

The charge of this purified complex was analyzed by using a linear 600-mL sodium perchlorate gradient, 0.0–2.0 M, at pH 7, with a 1 cm × 45 cm AG-50 (Na^+) column that had been calibrated by using cobalt complexes of various charges. The results (Figure 4) showed the charge of the complex to be 1+.

$NH_4TbEDTA$ was prepared by adding 2.9 mmol of ethylenediaminetetraacetic acid (EDTA) to 3.1 mmol of $TbCl_3 \cdot 6H_2O$, purified by chromatography on a 2.5 × 38 cm AG-1 (acetate) column with an NH_4OAc gradient (1600 mL, 0.0–4.0 M, pH 6.8), and lyophilized. TbHED3A was prepared with excess *N*-(2-hydroxyethyl)ethylenediaminetriacetic acid (HED3A), washed through an AG-1 (acetate) column with water to remove chloride ions and excess HED3A, and lyophilized. $NH_4CoEDTA$ (hexadentate) was a gift from Simon Yeh.

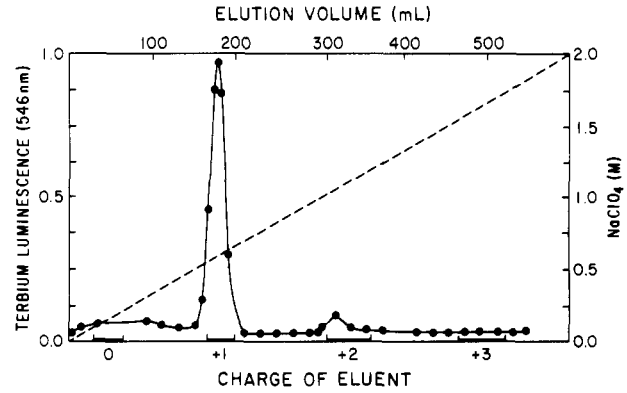

FIGURE 4: Chromatographic determination of the net charge of $TbBED2A^+$. A total of 52 mg of $TbBED2A^+$ was applied to a 1 cm × 45 cm AG-50 (Na^+ form) column and eluted with a 600-mL linear gradient of 0–2.0 M $NaClO_4$. Tb(III) luminescence was monitored at 546 nm, λ_{ex} 244 nm. Volume ranges indicated as corresponding to different net charges were determined by using the same column and an identical gradient to elute the following complexes: [Co(II)BED2A], $[Co(III)(en)_2Cl_2]^+$, $[Co(II)(H_2O)_6]^{2+}$, and $[Co(III)(en)_2(H_2O)_2]^{3+}$.

Sperm whale myoglobin (type II; Sigma Chemical Co.) was dissolved in distilled deionized water and dialyzed against water to remove salts. A slight excess of $K_3Fe(CN)_6$ was added to ensure complete conversion to the ferric form, and the solution was chromatographed on CM-Sephadex C-25. The procedure was essentially that of Hapner et al. (1968), except that all the protein was eluted with sodium phosphate buffer, pH 6.5, I = 0.1. The main peak was pooled and concentrated by dialysis against dry poly(ethylene glycol). The purified protein was then dialyzed against frequent changes of 0.1 N NaCl, until no phosphate could be detected by the method of Chen et al. (1956). Other procedures tried such as passage of the solution through a mixed-bed ion-exchange column and extensive dialysis against distilled water (Hapner et al., 1968) were not effective in removing all the phosphate (a step which was necessary to prevent precipitation of terbium phosphate).

The protein/NaCl solution was then dialyzed against deionized distilled water until the chloride concentration was below 3 mM (protein concentration was 560 μM, pH 6.1). The purified protein was stored as a frozen solution at −70 °C.

Samples for energy transfer were prepared by adding solutions of the terbium chelates to solutions of protein or $CoEDTA^-$, and adjusting pH with dilute NaOH; a Corning Model 12 pH meter and an Ingold micro combination pH electrode were used. Protein concentrations were determined by measuring the absorbance at 280 nm by using $\epsilon_{280} = 3.06 \times 10^4\ M^{-1}\ cm^{-1}$ (Hapner et al., 1968) or by forming the cyano complex and measuring the absorbance at 423 nm by using $\epsilon_{423} = 1.12 \times 10^5\ M^{-1}\ cm^{-1}$ (Hapner et al., 1968).

Experiments To Detect Probe Binding to Protein. It was important to establish that the observed processes simply involved electrostatic effects on the radial distribution of ions, rather than actual binding of the probes to the protein. Since such binding can be described by a set of equilibrium dissociation constants, it is easy to show that if the smallest dissociation constant (strongest binding) K_d is much greater than the total concentrations of donor and acceptor, binding would

not be important. In order to establish experimentally that binding was not significant, we simply chose a concentration of protein adequate to give easily measurable energy transfer and studied a series of samples with fixed protein concentration, in which the terbium chelate concentrations varied from a value well below that of the protein to a value well above. If binding were not important, then increasing the total concentration of terbium chelate, at fixed protein concentration, would not lead to a change in the observed lifetime of terbium but would yield a proportional increase in emission intensity. On the other hand, if binding were important, the resulting changes in charge and shape of the protein would lead to significant changes in terbium lifetime as a function of terbium concentration and also to a nonlinear increase in emission intensity.

To check for K_d's that would lead to significant binding for $\sim 10^{-3}$ M total chelate, a range from $\sim 2 \times 10^{-5}$ to $\sim 10^{-2}$ M chelate was tested. In fact, when 10^{-4} M myoglobin at pH 6 was studied with concentrations of $TbEDTA^-$ in excess of 1.5 mM, the terbium lifetime depended measurably on probe concentration (this effect diminished with increasing pH). $TbEDTA^-$ at 10^{-4} M was used for the experiments reported here, since no detectable binding occurred at this concentration. TbHED3A and $TbBED2A^+$ showed no evidence of protein binding at much higher concentrations, so 1 mM concentrations of these probes were used.

As an additional test for binding of the probes to the protein, the Soret absorbance of myoglobin was monitored at 408 nm in the presence and absence of each terbium chelate. A decrease in this absorbance has been shown to be an indicator of the loss of native structure of myoglobin (Friend & Gurd, 1979). The absorbance at 408 nm decreased by 6.8 ± 1.0% as the protein was titrated from pH 6 to pH 8, whether Tb(III) chelates were present or not. Addition of millimolar levels of any of the Tb(III) chelates led to an *increase* in the 408-nm absorbance of 2.3 ± 1.7% at pH 6, 7, or 8. These results suggest that there may be a subtle conformational change upon raising the pH to 8 and a smaller effect of varying the identity of the salts present. The uniformly small magnitude of the effect observed with the three probes over the whole pH range argues against any specific binding, and it seems likely that myoglobin retained essentially its native conformation throughout these experiments.

Critical Distance for Energy Transfer. R_0 was calculated according to eq 2 from myoglobin absorbance spectra (Figure 2) measured on a Hewlett-Packard 8450A UV/vis spectrophotometer and the corrected emission spectrum of $TbEDTA^-$ measured on a Perkin-Elmer MPF44B fluorescence spectrophotometer with a differential corrected spectra unit. The values used in eq 2 were $Q_0 = 0.2$ (Yeh & Meares, 1980), $\kappa^2 = {}^2/_3$, and $n = 1.33$. The value of Q_0 has an uncertainty of ±0.05 which is the principal source of uncertainty in the calculated values of R_0. The value of J, the spectral overlap integral (eq 3), varied from 4.33×10^{-14} (pH 6.0) to 5.16×10^{-14} cm^3 M^{-1} (pH 8.5), leading to R_0 values of 3.4 ± 0.1 and 3.5 ± 0.1 nm, respectively.

Terbium Lifetime Measurements. Rates of energy transfer were determined by measuring the luminescent lifetimes of each chelate in the absence and presence of protein at each pH. Tb(III) luminescence was excited by the 488-nm beam from an argon ion laser (CR-18, Coherent Radiation) which had been passed through a 488-nm dielectric interference filter. The excitation beam was modulated either by a chopper wheel which cut the excitation intensity to less than 1% in less than 20 μs or an acousto-optic modulator (Harris Corp., H211N-1-80 MOD) with a cutoff time of less than a microsecond. The emitted light was detected by a 56 DVP (Amperex) photomultiplier tube after passage through a potassium dichromate solution filter and two 546-nm dielectric interference filters (Optical Thin Films, Conway, NH).

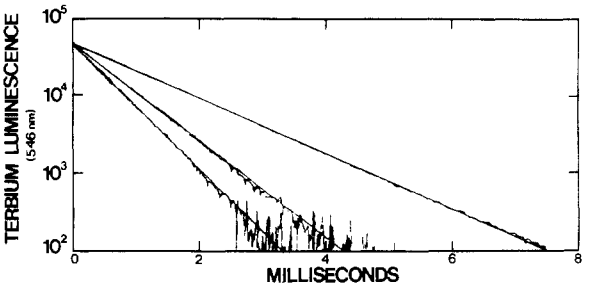

FIGURE 5: Typical semilogarithmic plots of the decay of Tb(III) luminescence. The straight lines superimposed on the experimental data are least-squares fits to $\ln [F(t)] = \ln [F(0)] - (t/\tau)$, where t is the time elapsed from the beginning of the decay and F is the relative luminescence intensity monitored at 546 nm. The ordinate indicates the number of photons detected. In each experiment, data were collected until the number of counts in the first channel was approximately equal to 7×10^4. (Upper trace) $TbEDTA^-$ in the absence of myoglobin ($\tau = 1.21$ ms); (middle trace) $TbEDTA^-$ plus 1.05×10^{-4} M met(aquo)myoglobin, pH 8.2 ($\tau = 0.708$ ms); (bottom trace) $TbEDTA^-$ plus 1.05×10^{-4} M met(aquo)myoglobin, pH 6.1 ($\tau = 0.544$ ms).

A combination of two discriminators (EG & G Model T105/N) and a dual or/nor gate (EG & G Model OR102/N) was used as a single channel analyzer to select only pulses in the desired energy range. These pulses, each corresponding to an emitted 546-nm photon, were counted by a Nicolet 1170 signal averager. Each sweep of the signal averager was triggered by the cutoff of the excitation beam.

The data (usually 256 points, 15 μs per address) were transferred to a microcomputer (Digital Equipment Corp., LSI-11/2) for analysis. Background (determined with a sample that was identical except for the absence of donor chelate) was subtracted, and the data were converted to logarithmic form and analyzed with a linear least-squares program to determine the luminescent lifetime.

For each sample a second-order rate constant for energy transfer was calculated from the measured luminescence lifetimes in the presence and absence of acceptor and the acceptor concentration (Yeh & Meares, 1980). Example data are plotted in Figure 5, along with the theoretical fits used to determine the lifetimes. All the rate constants reported here are based on single-exponential decays, as determined by a correlation coefficient of at least 0.999 for the fit of the logarithmic data to a straight line. Results of repeated measurements of the lifetime for identically prepared samples generally differed by no more than 2%.

In order to assure that no significant energy transfer occurred in the absence of the heme group, the effect of apomyoglobin (Wittenberg & Wittenberg, 1981) was studied. Over the pH range from 6 to 8, the lifetime of each terbium probe was the same (within 1%) in the presence or absence of 10^{-4} M apomyoglobin. This demonstrates that the probes are not quenched by ordinary protein side chains but only by chromophores.

Results and Discussion

Energy Transfer to Co(III)EDTA$^-$. Because the Tb(III) chelates used as probes can behave as weak acids, it was necessary to determine the pH range over which the charge of each probe remains constant. For this reason, the rate constant for energy transfer from each probe to $CoEDTA^-$ was

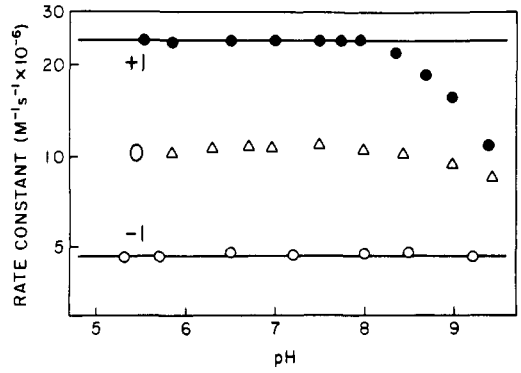

FIGURE 6: Semilogarithmic plot of second-order rate constants for energy transfer from terbium chelates to $CoEDTA^-$ as a function of pH. (Open circles) $TbEDTA^-$; (filled circles) $TbBED2A^+$; (triangles) TbHED3A. The horizontal lines are from eq 7 in the text by using unit charge for each of the charged chelates, a distance of closest approach $R_A + R_D = 0.7$ nm, and $k_0 = 10.5 \times 10^6$ M^{-1} s^{-1}. Each experiment contained 85.9 μM NaCl and 1 mM terbium chelate.

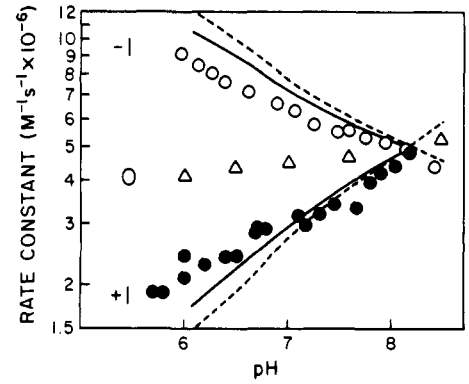

FIGURE 7: Semilogarithmic plot of second-order rate constants for energy transfer from terbium chelates to met(aquo)myoglobin as a function of pH. The donors were (open circles) $TbEDTA^-$, (filled circles) $TbBED2A^+$, and (triangles) TbHED3A. The solid lines were calculated for dipolar energy transfer according to eq 8 and 5, as described in the Appendix. Calculations using eq 8 and the nonlinear Poisson–Boltzmann approximation (see Appendix) agreed precisely with the solid lines above pH 6.2. The dashed lines were calculated for exchange-mediated energy transfer, according to eq 7. The charge of the protein varied from 5+ at pH 6 to 0 at pH 8.2.

measured as a function of pH. The results are shown in Figure 6. It can be seen that the charge of $TbEDTA^-$ remains constant over the whole pH range studied, TbHED3A remains neutral up to pH 8.5, and $TbBED2A^+$ has a unit charge below pH 8.0. Thus, below these indicated pH limits any pH dependence of the rate constants in the myoglobin experiments is due to changes in the protein, not in the probes.

It has been shown earlier (Meares et al., 1981) that energy transfer from Tb(III) chelates to $CoEDTA^-$ takes place by the exchange mechanism, so eq 7 is applicable. The lines plotted with the data points in Figure 6 are based on eq 7, assuming unit charges on the probes and a distance of closest approach (a) of each probe to $CoEDTA^-$ of 0.7 nm ($t = 0$). The value of a estimated from crystallographic data (Hoard et al., 1965; Weakliem & Hoard, 1959; Lee, 1967) and examination of molecular models is 0.8 (±0.2) nm. The close agreement with experiment shows that for this case the simple electrostatic model works well.

Energy Transfer to Met(aquo)myoglobin. Figure 7 shows the results for energy transfer from each of the terbium chelates to met(aquo)myoglobin. The upward trend in the rate constant for the neutral probe (TbHED3A) with increasing pH parallels the pH dependence of the protein absorption spectrum (Figure 2). Application of eq 4 using a value of 1.8 + 0.4 = 2.2 nm for the sum of the protein (Shire et al., 1974a) and probe radii leads to values of the distance of closest approach of the neutral donor and the acceptor at each pH value. These values vary only slightly over the pH range, from a minimum of 0.52 nm at pH 7.6 to a maximum of 0.54 nm at pH 6.0. The rate constant for energy transfer is dependent on the inverse third power of a but is much less sensitive to the value of t. The small variation in a over the pH range studied implies that no major changes in the accessibility of the heme occur with changing pH. These small values of a indicate that there can be direct contact between the donor chelate and the heme, and examination of molecular models of the crystal structure of myoglobin (Kendrew et al., 1960) suggests that there is enough room for a chelate of 0.8-nm diameter to make contact with the edge of the heme. Because of complications which occur at small donor–acceptor separations (Dexter, 1953; Stryer et al., 1982a), it seems unlikely that these a values accurately represent the minimum distances from the center of the terbium atom to the center of the heme iron.

The distance of closest approach a is calculated by assuming that energy transfer occurs by the dipolar mechanism. The present data offer no definitive way to determine whether the dipolar mechanism or the exchange mechanism is predominant in the observed energy transfer (although as discussed below the dipolar mechanism leads to better agreement with experimental results for electrostatic effects). It is not now possible to calculate a priori a rate constant for exchange-mediated energy transfer. However, the conclusion that the chelate collides with the heme does not depend on the assumption of either mechanism. If the dipolar mechanism predominates, a rate constant of the magnitude observed can only be explained by a very small distance of closest approach (~0.5 nm). On the other hand, if exchange-mediated energy transfer occurs, it must be caused by direct contact between donor and acceptor.

In comparing the pH dependence of the rate constants for the three different probes in Figure 7, the most striking feature is that all the rate constants converge near pH 8.2, the isoionic point of myoglobin (Shire et al., 1974a). Another immediate observation is that the points for the positive and negative probes are symmetrically disposed about the points for the neutral probe, indicating that both charged probes are responding to the same effects with increasing pH. The value of using three different probes is evident; this makes it possible to sort out conformational changes, as well as interactions that would be specific to one or another of the probes, from simple electrostatic effects.

While the ionic strength dependence of energy transfer was not studied extensively, some experiments were performed at various ionic strengths at pH 6 and pH 7. As predicted for simple electrostatic interactions, added salt (NaCl or $NaClO_4$) decreased the rate constant for the negative probe, increased the rate constant for the positive probe, and had no measurable effect on the neutral probe. In addition, it was found that at $NaClO_4$ concentrations above 30 mM, k_2 for the negative probe became lower than k_2 for the neutral probe, probably as a result of ClO_4^- binding to the protein. A similar effect was observed with NaCl at pH 6.

Comparison of Experimental with Theoretical Results. The curves shown in Figure 7 were obtained from eq 7 (dashed lines) or 8 (solid lines) by using eq 5 for $w(r)$. In addition, a similar curve was calculated by using the approximate solution of the nonlinear Poisson–Boltzmann equation (described in the Appendix) to calculate $w(r)$ for $TbEDTA^-$. At pH 6,

the Poisson–Boltzmann result was 2.5% lower than the curve shown in Figure 7, and above pH 6.2 the curves were indistinguishable.

The values of Z_A in each case were obtained from the titration data of Shire et al. (1974a). The quantity $(t + a) = R_A + R_D$, the sum of the donor and protein radii, was assumed to be 2.2 nm (Shire et al., 1974a) for both the dipolar and the exchange calculations, and for the dipolar calculation, the value of a was calculated from eq 4 as described above. The values of the ionic strength used for the calculations were those of the experimental samples, which were between 1.0 and 3.5 mM. Thus, all the quantities used in these calculations were independently measured. One quantity that is generally subject to uncertainty in the extended Debye–Hückel theory (eq 5) is the closest approach distance of the centers of the two ions $(t + a)$. Because a protein may not be accurately spherical (myoglobin is certainly not), and the charge distribution may not be centered at the geometric center of the molecule, this ambiguity is of special concern. Increasing the value of $(t + a)$ by 0.1 nm decreases the calculated k_2 value for $TbEDTA^-$ at pH 6.1 by about 4%.

The agreement between the theoretical curves and experimental results is not bad for eq 7 (the simple Boltzmann factor for the exchange mechanism), especially at the higher pH (smaller Z_A) values. It is even better for eq 8 (the dipolar expression, numerically integrated), regardless of which formula (eq 5 or 6) is used for the electrostatic potential of mean force. At the low pH end of the curve, where the deviation between theory and experiment is greatest, the difference corresponds to 0.5 charge unit, less than an 11% error. It should be noted that there are no adjustable parameters in these equations. The agreement between the curves derived from the two different expressions for the potential of mean force (eq 5 and 6) is an indication that for low surface charge densities such as myoglobin's $[e\psi/(kT) \approx 1]$ the simplifying assumptions leading to eq 5 are valid. The deviation of the theoretical curve from the experimental results at low pH (high Z_A) may be due to various effects not accounted for in this simple model, such as anion binding to the protein (Cameron et al., 1966) and to pH dependence of the effective protein radius.

The agreement between the experimental curves and the theory based on the simple model described above implies that the electrostatic effects are controlled by the overall net charge, rather than by specific local charges near the acceptor. This result may be partly due to the specific properties of myoglobin and partly due to general features of diffusion-enhanced energy transfer. The charges in myoglobin are fairly evenly distributed over the surface (based on a listing of coordinates for charged residues derived from data of Takano (1977), kindly provided by M. Flanagan, and examination of molecular models), and the region of the protein surface near the heme does not have an exceptional potential as compared to the rest of the protein.

Moreover, averaging can occur due to the through-space character of dipolar energy transfer and the long-range nature of electrostatic forces. In the case of dipolar energy transfer, the r^{-6} distance dependence (which becomes r^{-4} in the time-averaged radial distribution observed in the rapid-diffusion limit) leads to significant energy transfer taking place over a range of donor–acceptor separations up to a few nanometers (from eq 1 with $a = 0.53$ nm, about 85% of the dipolar energy transfer occurs at separations shorter than 1 nm). For millimolar ionic strength, the electrostatic potential due to an ion does not decrease much over such distances (Eisenberg & Crothers, 1979). As a result, the time-averaged potential encountered by the probe contains contributions from all charged residues on the protein. Rotational motion of the protein may also contribute to this averaging process. The rotational correlation time for myoglobin (Anderson et al., 1970; Johnson et al., 1977; Livingston et al., 1983) is approximately 6.3–10.3 ns, a time in which a donor chelate will have diffused a distance equal to about two myoglobin diameters.

It may be that in acceptors with more asymmetric charge distributions, the rates of energy transfer will be more sensitive to the details of the electrostatic potential in the immediate vicinity of a chromophore. This will certainly be true if the exchange mechanism of energy transfer predominates. Also, it is possible that for much larger macromolecules the total net charge will not bear the same simple relation to rates of energy transfer.

It is interesting that the difference between the theoretical curves for dipolar energy transfer and for the exchange mechanism (Figure 7) is much less than it would be for small molecules (Meares et al., 1981). The smaller difference is due to the large size of the acceptor molecule and the fact that electrostatic interactions take place, for the most part, over fairly long distances. As a result, the electrostatic potential 0.4 nm from the protein surface (the relevant distance for the exchange mechanism) is not very different from its value 1 nm from the surface (a distance within which most of the dipolar transfer occurs). This result is significant in that it implies that the use of a simple Boltzmann factor (as in eq 7) may give a useful estimate of the acceptor charge whether one knows the mechanism for energy transfer or not, and without the need for numerical integrations of the kind detailed in the Appendix.

Protein Charges. In measurements of the electric charge of a protein, ambiguity can arise from several sources. An accurate measure of the *proton* charge of a protein (i.e., the number of protons bound to or dissociated from titratable groups) can be made by pH titrations, provided that the isoionic point of the protein is accurately known and that all other acids and bases (e.g., CO_2 and phosphates) can be rigorously excluded (Nozaki & Tanford, 1967). But many proteins precipitate or denature near their isoionic pH, or in the zero salt conditions required to determine it. In addition, the experimental conditions of most interest for protein studies generally involve the presence of other ions (often with pK_a's near the pH of interest such as various buffers), which may bind to the protein and alter its net charge (and its titration behavior) considerably. Titration curves give no direct information about the overall protein charge in the presence of ion binding, although differential conductimetry has been used to obtain this quantity for some proteins (Sophianopoulos, 1973). Ion binding by a protein such as myoglobin is easy to observe by diffusion-enhanced energy transfer, because of its sensitivity to total protein charge.

Other Experiments. It is interesting that electron-transfer rate constants for reactions of myoglobin with small metal complexes (e.g., Antonini & Brunori, 1971; Cassatt et al., 1975; Mauk & Gray, 1979), like those for energy transfer reported here, are much smaller than the diffusion-controlled value of 10^9 M^{-1} s^{-1}. Therefore, the same equilibrium radial distribution of donors about each acceptor can be applied to either the electron-transfer or the energy-transfer experiments. By providing independent measures of the accessibility of redox centers and of the electrostatic contributions to protein–small molecule interactions, diffusion-enhanced energy transfer may

be helpful in the analysis of electron-transfer processes involving heme proteins.

Because of the mathematical similarities between dipolar energy transfer and dipolar broadening of NMR spectral lines (Abragam, 1961; Luz & Meiboom, 1964), it is also likely that the probes in Figure 1 (containing terbium, gadolinium, or other paramagnetic lanthanides) could be used in NMR studies of nonchromophoric groups in biological macromolecules.

Conclusion

We have found that diffusion-enhanced energy transfer from the three terbium chelates $TbEDTA^-$, TbHED3A, and $TbBED2A^+$ can be used to measure both the accessibility of a chromophoric group and the charge of the macromolecule that contains it. Under the conditions employed, the probes do not bind to the protein and apparently introduce no significant perturbations in its structure and electrostatic properties. Consequently, the relative rates of energy transfer from probes of different charges give a direct measure of the radial distribution of ions about the protein and therefore of the electrostatic potential. The symmetry of the effects observed with the negative and positive probes and comparison with the results obtained with the neutral probe indicate that the changes measured are due to simple electrostatic interactions.

In order for diffusion-enhanced energy transfer experiments to yield useful information in a straightforward way, it is essential to check for binding of the probes to the energy acceptor as described above. Use of lifetime measurements to determine rates of energy transfer is also important (although in principle steady-state intensity measurements can be used) because this helps to eliminate interference from organic fluorescence and scattering and because the single-exponential character of the luminescence decays serves as a check on the homogeneity of the donor environment (characteristic of the rapid-diffusion limit).

The basic approach described here can be readily extended to more complex situations. Many proteins have colored substrates or prosthetic groups, and others can be chemically modified to add chromophoric groups. Many DNA-binding dyes are excellent energy acceptors, and biological membranes may contain natural chromophores or added dyes [e.g., see Stryer et al. (1982b) and Thomas & Stryer (1982)]. For these systems, diffusion-enhanced energy transfer offers a way to make accurate, rapid measurements that have a straightforward interpretation in terms of chromophore accessibility and charge interactions.

Acknowledgments

We thank Simon Yeh for providing $CoEDTA^-$, Dayton Reardan for preparing $TbEDTA^-$, Margaret Flanagan for providing a listing of pK_a's and the coordinates of charged groups in myoglobin, and James Matthew, D. A. McQuarrie, and J. E. Keizer for helpful discussions.

Appendix

Numerical Calculation of the Effect of Electrostatic Interactions on the Rate Constant for Diffusion-Enhanced Energy Transfer from a Spherical Donor to an Acceptor Located off the Center of an Impenetrable Sphere. The model used is illustrated in Figure 3. A spherical coordinate system is chosen, with its origin at the center, O, of the sphere representing the protein. Angle θ is chosen to be 0 when OA and OD coincide. The rate of energy transfer is dependent on the inverse sixth power of the donor–acceptor separation r_{et} (the length of AD). This distance is given by

$$r_{et} = (r^2 + t^2 - 2rt\cos\theta)^{1/2} \quad \text{(A1)}$$

The second-order rate constant for diffusion-enhanced energy transfer is given by

$$k_2 = \frac{0.6023R_0^6}{\tau_0}\int_0^{2\pi}\int_0^{\pi}\int_{a+t}^{\infty}(r^2 + t^2 - 2rt\cos\theta)^{-3}\exp[-w(r)/(kT)]r^2\sin\theta\,dr\,d\theta\,d\phi \quad \text{(A2)}$$

where τ_0 is in s, R_0 and r are in nm, and k_2 is given in M^{-1} s^{-1}. The function $w(r)$ can be taken as either the extended Debye–Hückel expression (eq 5) or the more elaborate expression of Ohshima et al. described below. In either case, in the model used, $w(r)$ is a function only of r.

Integration over ϕ yields a factor of 2π due to the cylindrical symmetry of the problem. What is required then is a numerical integral over r and θ. This integration was performed by using a Romberg extrapolation method (modified from a Digital Equipment Corp. Scientific Subroutines program), with each value in the Romberg iteration scheme evaluated by the trapezoidal rule. The value of the integrand at each point in the integration over θ was determined by carrying out the integration over r with θ fixed. The Romberg iteration scheme was repeated, with progressively smaller intervals, until an accuracy within a predetermined error was reached. The value of this error was decreased until further decrease produced no significant change in the calculated result. The upper limit in the integral over r was taken as 100 nm. Larger values for this limit made no difference in the calculated result.

Use of Approximate Analytic Solution to the Nonlinear Poisson–Boltzmann Equation. Oshima et al. (1982) have found relations between electrostatic potential and surface charge density which yield results in very close agreement with numerical solutions of the nonlinear Poisson–Boltzmann equation. Their eq 24 provides a method for calculating the surface potential from the surface charge density $\sigma = Z_A e/4\pi R_A^2$. Their eq 49 then provides the electrostatic potential $\psi(r)$ used in eq 6 above.

Registry No. BED2A, 5616-21-7; *N,N'*-bis(2-hydroxyethyl)-ethylenediamine, 4439-20-7; $BrCH_2CO_2H$, 79-08-3; $TbBED2A^+$, 87698-05-3; $TbEDTA^-$, 15158-65-3; TbHED3A, 75180-61-9; $CoEDTA^-$, 87698-06-4.

References

Abragam, A. (1961) *The Principles of Nuclear Magnetism*, Chapter 4, pp 122–124, Oxford University Press, London.

Anderson, S. R., Brunori, M., & Weber, G. (1970) *Biochemistry 9*, 4723–4729.

Antonini, E., & Brunori, M. (1971) *Hemoglobin and Myoglobin in Their Reactions with Ligands*, pp 340–342, American Elsevier, New York, NY.

Cameron, B. F., Hanania, G. I. F., & Tayim, H. (1966) in *Hemes and Hemoproteins* (Chance, B., Estabrook, R., & Yonetani, T., Eds.) p 263, Academic Press, New York.

Cassatt, J. C., Marini, C. P., & Bender, J. W. (1975) *Biochemistry 14*, 5470–5475.

Chaberek, S., & Bersworth, F. C. (1953) *Science (Washington, D.C.) 118*, 280.

Chen, P. S., Jr., Toribara, T. Y., & Warner, H. (1956) *Anal. Chem. 28*, 1756–1758.

Dexter, D. L. (1953) *J. Chem. Phys. 21*, 836–850.

Eisenberg, D., & Crothers, D. (1979) *Physical Chemistry with Applications to the Life Sciences*, p 37, Benjamin/Cummings, Menlo Park, CA.

Förster, T. (1948) *Ann. Phys. (Leipzig) 2*, 55–75.

Friend, S. H., & Gurd, F. R. N. (1979) *Biochemistry 18*, 4612-4619.
Hapner, K. D., Bradshaw, R. A., Hartzell, C. R., & Gurd, F. R. N. (1968) *J. Biol. Chem. 243*, 683-689.
Hoard, J. L., Lee, B., & Lind, M. D. (1965) *J. Am. Chem. Soc. 87*, 1612-1613.
Johnson, M. E., Fung, L. W.-M., & Ho, C. (1977) *J. Am. Chem. Soc. 99*, 1245-1250.
Kendrew, J. C., Dickerson, R. E., Strandberg, B. E., Hart, R. G., Davis, D. R., Phillips, D. C., & Schore, V. C. (1960) *Nature (London) 185*, 422-427.
Lee, B. (1967) Ph.D. Thesis, Cornell University.
Livingston, D. J., La Mar, G. N., & Brown, W. D. (1983) *Science (Washington, D.C.) 220*, 71-73.
Luz, Z., & Meiboom, S. (1964) *J. Chem. Phys. 40*, 2686-2692.
Matthew, J. B., Friend, S. H., Botelho, L. H., Lehman, L. D., Hanania, G. I. H., & Gurd, F. R. N. (1978) *Biochem. Biophys. Res. Commun. 81*, 416-421.
Mauk, A. G., & Gray, H. B. (1979) *Biochem. Biophys. Res. Commun. 86*, 206-210.
McClanahan, C. J. (1982) Dissertation, University of California, Davis.
McLaughlin, S. (1977) *Curr. Top. Membr. Transp. 9*, 71-144.
Meares, C. F., & Rice, L. S. (1981) *Biochemistry 20*, 610-617.
Meares, C. F., Yeh, S. M., & Stryer, L. (1981) *J. Am. Chem. Soc. 103*, 1607-1609.
Nozaki, Y., & Tanford, C. (1967) *Methods Enzymol. 11*, 715-734.
Olivares, W., & McQuarrie, D. A. (1975) *Biophys. J. 15*, 143-162.
Oshima, H., Healy, T. W., & White, L. R. (1982) *J. Colloid Interface Sci. 90*, 17-26.
Rice, L. S., & Meares, C. F. (1982) *Biochem. Biophys. Res. Commun. 105*, 51-56.
Rice, S. A., & Nagasawa, M. (1961) *Polyelectrolyte Solutions*, Academic Press, London.
Scheraga, H. A., Katchalsky, A., & Alterman, Z. (1969) *J. Am. Chem. Soc. 91*, 7242-7249.
Shire, S. J., Hanania, G. I. H., & Gurd, F. R. N. (1974a) *Biochemistry 13*, 2967-2974.
Shire, S. J., Hanania, G. I. H., & Gurd, F. R. N. (1974b) *Biochemistry 13*, 2974-2979.
Sophianopoulos, A. J. (1973) *Methods Enzymol. 27*, 557-590.
Stryer, L., Thomas, D. D., & Meares, C. F. (1982a) *Annu. Rev. Biophys. Bioeng. 11*, 203-222.
Stryer, L., Thomas, D. C., & Carlsen, W. F. (1982b) *Methods Enzymol. 81*, 668-678.
Takano, T. (1977) *J. Mol. Biol. 110*, 537-568.
Thomas, D. D., & Stryer, L. (1982) *J. Mol. Biol. 154*, 145-157.
Thomas, D. D., Carlsen, W. F., & Stryer, L. (1979) *Proc. Natl. Acad. Sci. U.S.A. 75*, 5746-5750.
Weakliem, H. A., & Hoard, J. L. (1959) *J. Am. Chem. Soc. 81*, 549-555.
Wittenberg, J. B., & Wittenberg, B. A. (1981) *Methods Enzymol. 76*, 34.
Yeh, S. M., & Meares, C. F. (1980) *Biochemistry 19*, 5057-5062.

Raman Spectroscopic Study of Age-Related Structural Changes in the Lens Proteins of an Intact Mouse Lens†

Y. Ozaki,* A. Mizuno, K. Itoh, M. Yoshiura, T. Iwamoto, and K. Iriyama

ABSTRACT: Age-related structural changes in the lens proteins of a normal mouse lens have been monitored in situ by laser Raman spectroscopy. The Raman spectrum of an ICR-strain mouse lens nucleus showed virtually no change in the 550–850- and 900–1800-cm^{-1} regions as the mouse aged. Lens aging, however, did cause a significant intensity decrease of the Raman band at 880 cm^{-1} due to tryptophan residues, and the intensity decrease seems to be stepwise. This observation implies that a microenvironmental change of tryptophan residues takes place twice at different places of the lens proteins during normal aging. Particularly striking is that the intensity decrease of the band at 880 cm^{-1} proceeds in parallel with that of the Raman band at 2579 cm^{-1} due to a SH stretching mode for the first 4 months. Thus, the first microenvironmental change of tryptophan residues seems to be correlated with the formation of S–S bonds. In contrast to tryptophan residues, no evidence was observed of a microenvironmental change in tyrosine residues. In this respect, the structural changes of lens proteins in aging are sharply distinct from those in lens opacification, in which tyrosine as well as tryptophan residues undergo microenvironmental changes [Itoh, K., Ozaki, Y., Mizuno, A., & Iriyama, K. (1983) *Biochemistry 22*, 1773-1778]. The relative intensity of the band at 3390 cm^{-1} due to an OH stretching mode of lens water fell rapidly for the first 4 months and then decreased very gradually. The observation clearly exhibits the process of lens dehydration. The age-dependent profile of the relative intensity of the OH stretching mode is similar to that of the SH stretching mode, implying that lens dehydration is also related to the 2SH → S–S conversion.

The predominant dry components of a mammalian lens are three structural proteins called α-, β-, and γ-crystallins, and their combined weight accounts for approximately 33% of the total weight of the lens (Cotlier, 1981). A disorder in the physicochemical arrangement of the lens proteins brings about lens aging or opacification. The well-known phenomena occurring to the lens proteins during such aging and opacification are lens dehydration or hydration, the formation of protein aggregates, and the chemical modification of protein subgroups (Kinoshita, 1974; Harding & Dilley, 1976; Cotlier, 1981; Bettelheim & Siew, 1982). To understand lens aging or

† From the Division of Biochemistry (Y.O., M.Y., T.I., and K.I.) and the Department of Ophthalmology (A.M.), The Jikei University School of Medicine, Minato-ku, Tokyo, Japan 105, and the Department of Chemistry, School of Science and Engineering, Waseda University, Shinjuku-ku, Tokyo, Japan 160 (K.I.). *Received May 24, 1983.*

0006-2960/83/0422-6254$01.50/0